

Extragenic Suppressors of the *nimX2^{cdc2}* Mutation of *Aspergillus nidulans* Affect Nuclear Division, Septation and Conidiation

Sarah Lea McGuire, Dana L. Roe, Brett W. Carter, Robert L. Carter, Sean P. Grace, Peyton L. Hays, Gene A. Lang, Jerry L. C. Mamaril, Allison T. McElvaine, Angela M. Payne, Melanie D. Schrader, Suzanne E. Wahrle and Chad D. Young

Department of Biology, Millsaps College, Jackson, Mississippi 39210

Manuscript received April 5, 2000

Accepted for publication August 17, 2000

ABSTRACT

The *Aspergillus nidulans* NIMX^{CD₂} protein kinase has been shown to be required for both the G₂/M and G₁/S transitions, and recent evidence has implicated a role for NIMX^{CD₂} in septation and conidiation. While much is understood of its G₂/M function, little is known about the functions of NIMX^{CD₂} during G₁/S, septation, and conidiophore development. In an attempt to better understand how NIMX^{CD₂} is involved in these processes, we have isolated four extragenic suppressors of the *A. nidulans nimX2^{cdc2}* temperature-sensitive mutation. Mutation of these suppressor genes, designated *snxA*-*snxD* for suppressor of *nimX*, affects nuclear division, septation, and conidiation. The cold-sensitive *snxA1* mutation leads to arrest of nuclear division during G₁ or early S. *snxB1* causes hyperseptation in the hyphae and sensitivity to hydroxyurea, while *snxC1* causes septation in the conidiophore stalk and aberrant conidiophore structure. *snxD1* leads to slight septation defects and hydroxyurea sensitivity. The additional phenotypes that result from the suppressor mutations provide genetic evidence that NIMX^{CD₂} affects septation and conidiation in addition to nuclear division, and cloning and biochemical analysis of these will allow a better understanding of the role of NIMX^{CD₂} in these processes.

THE filamentous fungus *Aspergillus nidulans* has proven to be a useful genetic system both for the study of cell cycle control and for the study of signals that establish patterns of cell growth and differentiation. It has long been recognized that nuclear division in *A. nidulans* is linked to septation and asexual development (FIDDY and TRINCI 1976; MIRABITO and OSMANI 1994); however, the molecular and genetic nature of these relationships has only recently begun to be elucidated. Recent studies have afforded a significant understanding of the molecular regulation of the G₂/M transition of *A. nidulans* (for a review, see YE and OSMANI 1997). Two protein kinases, the NIMX^{CD₂} protein kinase and the NIMA protein kinase, are coordinately required to initiate mitosis in *A. nidulans* (OSMANI and YE 1996; YE *et al.* 1996), and their rapid inactivations are essential for progression through mitosis (GLOTZER *et al.* 1991; PU and OSMANI 1995). In addition, both protein kinases appear to be the targets of checkpoint regulation (YE *et al.* 1997a, 1998). Evidence exists indicating that NIMA may be required for the proper localization of NIMX^{CD₂}/cyclinB to initiate mitosis (WU *et al.* 1998).

In addition to its mitosis-promoting function, NIMX^{CD₂} is required for the G₁/S transition; however, little is known about its G₁/S function and no G₁-specific genes

that regulate NIMX^{CD₂} have been identified in *A. nidulans*. S-M checkpoint control in response to incomplete DNA replication and DNA damage functions via regulation of phosphorylation of the Tyr-15 residue of NIMX^{CD₂} (YE *et al.* 1996; YE and OSMANI 1997). Loss of such checkpoint control regulation over mitosis can also cause defects in DNA rereplication after mitosis (DESOUZA *et al.* 1999). Triggered by the NIMQ^{MCM₂} DNA licensing factor (YE *et al.* 1997b), checkpoint control over mitotic function at the G₁/S transition is transferred from the anaphase promoting complex/cyclo-some (APC/C; LIES *et al.* 1998; YE *et al.* 1998; ZACHARIEA and NASMYTH 1999) to include Tyr-15 phosphorylation of NIMX^{CD₂}. One function of the APC/C is to ubiquitinate cyclinB in late mitosis and G₁, thus ensuring that NIMX^{CD₂} is inactive during these times. Thus, the activity of NIMX^{CD₂}/cyclinB is highly regulated at all phases of the nuclear division cycle, but many of the details of this regulation are still not understood in *A. nidulans*. Identification of proteins that interact with NIMX^{CD₂} will allow a better understanding of its regulation.

Vegetative hyphae of *A. nidulans* grow by apical extension of a germ tube from a single conidium. As the hypha extends, the nuclei undergo repeated mitotic divisions. Beginning with the third nuclear division, crosswalls called septa are typically laid down at uniform intervals along the vegetative hyphae (HARRIS *et al.* 1994; KAMINSKYJ and HAMER 1998), producing a multinucleate syncytium. The formation of septa is the equiv-

Corresponding author: Sarah Lea McGuire, Millsaps College, P.O. Box 150305, 1701 N. State St., Jackson, MS 39210.
E-mail: mcguisl@millsaps.edu

alent of cytokinesis and is dependent upon cell size, mitosis, and nuclear positioning (WOLKOW *et al.* 1996). Cytokinesis is tightly coupled with mitosis in many organisms (SATTERWHITE and POLLARD 1992), and cyclin-dependent kinase activity is believed to coordinate cytokinesis with mitosis (SATTERWHITE *et al.* 1992). In *A. nidulans*, high levels of NIMX^{CDC2} activity are required for septum formation. In the *nimX^{cdc2AF}* strain, NIMX^{CDC2} is unable to be phosphorylated at positions 14 and 15, leading to increased NIMX^{CDC2} activity and premature septation (HARRIS and KRAUS 1998). Septation in this strain also occurs inappropriately in the conidiophore stalk, resulting in defects in conidiophore development (YE *et al.* 1999). Recent evidence has shown that mutations in *bimA^{APC3}*, which encodes part of the APC/C, indirectly affect septation by leading to errors in DNA metabolism (WOLKOW *et al.* 2000). Thus, both septation and nuclear division are affected by the APC/C and the activity of NIMX^{CDC2}, but little is understood of the molecular and genetic relationships between the APC/C, NIMX^{CDC2}, and septation.

The molecular mechanisms controlling conidiophore development have been extensively studied (for a review, see ADAMS *et al.* 1998). Recent work has shown that NIMX^{CDC2} is regulated by the BrlA transcriptional regulator, which cues the switch from hyphal growth to conidiophore development, and that the *nimX^{cdc2AF}* strain has defects in conidiophore development (YE *et al.* 1999). Proper function of NIMX^{CDC2} is therefore essential for nuclear division, septation, and conidiophore development. Elucidation of the regulation of NIMX^{CDC2} in *A. nidulans* will allow a better understanding of how these processes are integrated at the molecular level.

Three temperature-sensitive *nimX* alleles, *nimX1*, *nimX2*, and *nimX3*, arrest nuclei in interphase (OSMANI *et al.* 1994). *nimX1* arrests in G₂, while *nimX3* arrests in both G₁ and G₂. The arrest point of *nimX2* is less clear, with at least some cells arresting in G₂; however, the homologous mutation in *Schizosaccharomyces pombe*, *cdc2-45*, leads to G₁ arrest (MACNEILL *et al.* 1991). To identify genes that interact with NIMX^{CDC2} in *A. nidulans*, we generated a series of extragenic suppressors of the *nimX2* temperature-sensitive allele. Here we describe the genetic and phenotypic characterization of mutants representing four genes that interact with NIMX^{CDC2}. We call these genes *snxA-snxD*, for suppressor of *nimX*. *snxA1* affects nuclear division and results in a block during G₁ or early S at the restrictive temperature, *snxB1* causes aberrant hyphal septation and increased sensitivity to hydroxyurea, *snxC1* leads to aberrant conidiophore septation and development, and *snxD1* leads to hydroxyurea sensitivity and slight septation defects. Characterization of these mutations and cloning of the genes will allow a better understanding of the molecular control of NIMX^{CDC2} and how its control affects nuclear division, septation, and asexual development.

TABLE 1

A. *nidulans* strains

Strain	Genotype
SO64 ^a	<i>riboA1; nimX2 wA2; nicB8</i>
SO65 ^a	<i>riboA1 yA2 pyroA4; nimX3 wA2</i>
SO69 ^a	<i>riboA1 yA2; nimX1; nicB8</i>
R153 ^a	<i>pyroA4; wA2</i>
A612 ^a	<i>Acra1; riboB2 chaA1</i>
A154 ^b	<i>adE20biA1; wA2 cnxE16; sc12; methG1; nicA2; lacA1; choA1; chaA1</i>
SWJ031 ^b	<i>nimG10; pyrG89; nicA2; chaA1</i>
SWJ313 ^b	<i>nimR21 cnxE16; pabaA1; chaA1</i>
SWJ108 ^b	<i>nimT23 cnxE16; nicA2; pabaA1; yA2</i>
SWJ195 ^b	<i>pabaA1; nimE6 wA2</i>
SWJ198 ^b	<i>nimE6; methB3; pyroA4</i>
SWJ298 ^b	<i>pyrG89; nicA2; chaA1</i>
ΔANKA ^a	<i>pyrG89; ΔankA wA3; pyroA4</i>
MDS250 ^c	<i>riboA1; snxA1 nimX2 wA2; nicB8</i>
RLC1 ^d	<i>pyrG89 riboA1; snxA1 wA2</i>
RLC4 ^d	<i>pyrG89; snxA1 wA2; nicA2</i>
BC7 ^e	<i>snxA1 wA2; nicB8; riboB2</i>
BC16 ^e	<i>riboA1; snxA1</i>
BC26 ^e	<i>snxA1; riboB2</i>
CY17 ^e	<i>riboA1; nimX2 wA2; snxB1 nicB8</i>
BC70 ^e	<i>riboA1; snxB1</i>
BC72 ^e	<i>snxB1 nicB8; riboB2</i>
MCG1 ^f	<i>pyrG89; snxB1</i>
CY1228 ^e	<i>snxC1 riboA1; nimX2 wA2; nicB8</i>
BC52 ^e	<i>snxC1; riboB2</i>
BC60 ^e	<i>snxC1; nicB8; chaA1</i>
S220 ^e	<i>riboA1; nimX2 wA2; snxD1 nicB8</i>
BC76 ^e	<i>riboA1; snxD1 nicB8</i>
BC81 ^e	<i>riboA1; snxD1</i>
BC93 ^e	<i>wA2; snxD1; riboB2</i>
MCG3 ^g	<i>pyrG89; ΔankA; snxB1</i>
MCG4 ^g	<i>pyrG89 snxC1; ΔankA; pyroA4</i>
MCG5 ^g	<i>nimT23 cnxE16; snxB1</i>
MCG6 ^g	<i>riboA1 snxC1; nimT23; yA2</i>

^a Obtained from Dr. Stephen A. Osmani, Henry Hood Research Program, Weis Center for Research, Geisinger Clinic, Danville, PA 17822.

^b Obtained from Dr. Stephen W. James, Gettysburg College, Gettysburg, PA 17325.

^c This study; parental extragenic suppressor isolated from mutagenesis of SO64.

^d This study; progeny from SWJ298 × BC7.

^e This study; progeny from A612 × parental suppressor strain.

^f This study; progeny from SWJ298 × BC70.

^g This study; double-mutant progeny (see MATERIALS AND METHODS).

MATERIALS AND METHODS

Strains and growth conditions: Strains used in this study are listed in Table 1. Media used were the following: rich media, MG (2% malt extract, 2% glucose, 0.2% peptone, trace elements, and vitamins) or YG (1% glucose, 0.5% yeast extract, trace elements, and vitamins) and minimal media (MM; 1% glucose, potassium chloride, nitrate salts, and trace elements). Trace elements, potassium chloride, nitrate salts, and vitamins are described in the appendix to KAUFER (1977). Agar (1.8%)

was added for solid medium. Genetic techniques were as described in HARRIS *et al.* (1994), except that heterokaryon formation was accomplished by plating strains containing complementary auxotrophic markers 1 cm apart on rich media, incubating at 32° for 2 days, and transferring the zone of mixed mycelia to an MM plate at 32°. When heterokaryotic growth was evident, heterokaryons were subcultured onto MM plates. Spontaneous diploids were isolated as described in ENGLE (1997).

Mutagenesis and identification of extragenic suppressors with independent phenotypes: Mutagenesis of strain SO64 (*nimX2*) was accomplished as described in HOLT and MAY (1996). Revertant colonies (2500) were isolated to single colony three times and retested for growth at 42° as well as for growth at 20° for 5–7 days (to test for cold sensitivity) or for growth at 32° on solid rich media containing 4% dimethylsulfoxide (DMSO; 4 days), 15 mM hydroxyurea (HU; 4 days), 0.01% methyl methanesulfonate (5 days), or 4 µg/ml benomyl (BEN; 5 days). Sexual crosses between strain A612 and all revertants that had an additional independent phenotype were performed as described (HARRIS *et al.* 1994) to determine if the reversion mutation was intragenic or extragenic and if the independent phenotype cosegregated with reversion. Strains containing extragenic suppressor mutations that cosegregated with the independent phenotype were assigned to linkage group by parasexual genetic analysis (PONTECORVO *et al.* 1953; KAUFER 1977) using diploids made between mitotic mapping strain A154 and strains carrying the suppressor mutation but not the *nimX2* mutation (BC16, BC70, BC52, and BC76). Haploidization was accomplished as described in HOLT and MAY (1996). Haploid colonies were replica plated onto solid rich media under the appropriate selective conditions to test for specific chromosome markers and the suppressor mutation. Mutations were assigned to linkage group by their linkage with known chromosomal markers (*snxA1*, *snxB1*, *snxC⁺*, and *snxD1*) as described in ENGLE (1997). Because *snxC1* is dominant, it could not be mapped by following linkage of the *snxC1* mutation with chromosomal markers. We thus mapped *snxC* by following cosegregation of the *snxC⁺* allele with chromosomal markers in haploid segregants. The diploids generated with strain A154 were also used to determine dominance or recessiveness of the suppressor mutations by analyzing diploid growth under selective conditions.

Generation and screening of double mutants: To generate double mutants containing *snxB1* or *snxC1* and either $\Delta ankA^{we1}$ or *nimT23^{delc25}*, the following crosses were made: SWJ108 × BC72, SWJ108 × BC50, $\Delta ANKA$ × BC72, and $\Delta ANKA$ × BC52. Progeny from each cross were tested for growth under restrictive conditions for each mutation. The *nimT23* mutation confers temperature sensitivity at 43°, while the *ankA* deletion causes sensitivity to 5 mM hydroxyurea. *SnxB1* mutants can form a small colony on 5 mM HU but are sensitive to 15 mM HU, and *snxC1* confers an inability to conidiate in the presence of 4% DMSO. For each cross, four classes of progeny were clearly identifiable: two parental single-mutant classes and two recombinant classes (one wild type and another distinctly different from either parent and wild type). To determine if progeny in the fourth class were double mutants, five progeny from each cross were streaked to single colony twice, retested for growth under restrictive conditions, and crossed to a wild-type strain (A612). The appearance of both single-mutant phenotypes among the progeny indicated that these were double mutants.

Staining, microscopy, and measurements: To visualize nuclei and septa, conidia were incubated as described in HARRIS *et al.* (1994) and fixed and stained with the DNA-specific dye 2,4-diamidino-2-phenylindole (DAPI) as described (OSMANI *et al.* 1990). Septa were simultaneously stained with nuclei

by including 4 µg/ml fluorescent brightener 28 (calcofluor; Sigma Chemical Co., St. Louis) in the staining mix. Fluorescence microscopy was performed using a Nikon Alphaphot microscope and a Leica DM-LB microscope. Subapical cell length, defined as the distance between adjacent septa measured at the junction between the septa and the lateral hyphal wall, was measured using SPOT Advanced software (Diagnostic Instruments) calibrated with an ocular micrometer. At least 50 subapical cells were analyzed for each strain. The nonparametric Mann-Whitney test was used to determine the statistical significance of the differences in subapical cell length. The percentage of cells that septate early was determined by counting the number of germlings with four nuclei that contained septa; 100 randomly selected germlings containing four nuclei were counted for each strain.

Reciprocal shift experiments: Reciprocal shift experiments to determine at which stage of interphase *snxA1* cells arrest were performed as described (BERGEN *et al.* 1984; OSMANI *et al.* 1994). Conidia from strains BC7 and MDS250 were first arrested in S phase by inoculation onto coverslips in rich media containing 25 mM HU and incubated 6.5 hr at 32°. The coverslips were either fixed (as a control) or transferred to 32° rich media in the absence of HU or to precooled 20° rich media in the absence of HU, incubated for 25 hr at 20°, and fixed. For the reciprocal experiment, conidia were inoculated into precooled 20° rich media in the absence of HU, incubated for 25 hr at 20°, either fixed (as a control) or transferred to 32° in the presence or absence of 25 mM HU, incubated at 32° for 3 hr, and fixed. These experiments were also performed using 19-hr incubations at 20°. Coverslips were stained with DAPI and the number of nuclei per germling determined.

RESULTS

Isolation of *nimX2* revertants: The *nimX2* mutation was chosen for these experiments because it arrests nuclei in G₁ or G₂ at the restrictive temperature of 42° (OSMANI *et al.* 1994), resulting in an inability to form colonies at this temperature. Suppressor mutants were isolated after treatment of conidia with NQO by plating survivors onto rich media followed by incubation at 42°. Under these conditions, control treatment with no NQO (solvent only) resulted in no colony formation, whereas conidia treated with 4–8 µg/ml NQO produced viable colonies. These heat-insensitive colonies were streaked to single colony three times and tested for growth at 32° and 42°. To facilitate future genetic analysis and cloning, we tested these revertants following each streak to single colony for the presence of an easily scorable selectable phenotype. A total of 2500 revertants were isolated and scored for growth inhibition at 20° (cold sensitivity, Cs⁻) and for growth inhibition in the presence of 4% DMSO, 15 mM HU, 0.01% methyl methanesulfonate (MMS), and 4 µg/ml BEN. A total of 22 revertants were Cs⁻, 2 were sensitive to DMSO, 3 were sensitive to HU, 1 was sensitive to MMS, and 12 were sensitive to BEN.

Each of the revertants that possessed an additional phenotype was crossed to strain A612, which has a wild-type *nimX* allele, to determine if the mutation leading to reversion was intragenic or extragenic. The presence

TABLE 2

Analysis of progeny from crosses of extragenic suppressor strains \times A612

Strain	No. of progeny in phenotypic class ^a			
	ts ⁺ /cs ⁺	ts ⁺ /cs ⁻	ts ⁻ /cs ⁺	ts ⁻ /cs ^{-b}
CY206	50	33	4	13
MDS250	204	144	46	0
MDS261	136	24	15	0
MDS527	32	41	14	12
MDS545 ^c	82	1	11	0
MDS637	54	10	27	10
S104	25	12	3	10

Strain	ts ⁺ /hu ⁺	ts ⁺ /hu ⁻	ts ⁻ /hu ⁺	ts ⁻ /hu ^{-b}
CY17	110	34	56	0
S220	59	26	15	0

Strain	ts ⁺ /DMSO ⁺	ts ⁺ /DMSO ⁻	ts ⁻ /DMSO ⁺	ts ⁻ /DMSO ^{-b}
CY1228	44	42	18	0

Crosses between strains carrying various suppressor mutations and strain A612 were made and progeny from each cross were tested for the presence of recombinant phenotypes. ts, temperature sensitive; cs, cold sensitive.

^a Indicates the number of progeny in the following phenotypic classes from the crosses listed: ts⁺, growth at 42°; ts⁻, lack of growth at 42°; cs⁺, growth at 20°; cs⁻, lack of growth at 20°; hu⁺, growth in the presence of 15 mM hydroxyurea; hu⁻, inhibited growth in the presence of 15 mM hydroxyurea; DMSO⁺, growth in the presence of 4% dimethylsulfoxide; DMSO⁻, inhibited growth/lack of conidiation in the presence of 4% dimethylsulfoxide.

^b Progeny in this column indicate lack of cosegregation of suppression with the additional phenotype.

^c This suppressor strain had only a marginal Cs⁻ phenotype that was difficult to score.

of heat-sensitive colonies in the progeny indicated that suppression of the *nimX2* mutation was extragenic (Table 2). Of the 40 revertant colonies with independent phenotypes tested, 15 contained extragenic suppressor mutations. Of these 15, 7 were Cs⁻, 2 were HU⁻, and 2 were DMSO⁻. The crosses also allowed a determination of whether the extragenic suppressor mutations cosegregated with the additional phenotypes possessed by the suppressor strains. Four BEN⁻ extragenic suppressor strains were also identified, but each of these contained extragenic suppressor mutations that did not cosegregate with the independent phenotype (data not shown). Of the six strains that contained cosegregating extragenic suppressors, MDS250 (Cs⁻), CY17 (HU⁻), CY1228 (DMSO⁻), and S220 (HU⁻) had clear suppressor and additional phenotypes and were used for further study. MDS261 was an extremely weak suppressor and MDS545 had only a marginal Cs⁻ phenotype that could not be scored reliably.

Linkage analysis: To determine the number of genes

TABLE 3

Linkage testing of extragenic suppressors

Suppressor mutation from strain	MDS250	CY17	CY1228	S220
S220	+	+	+	
CY1228	+	+		
CY17	+			

Crosses between strains carrying various suppressor mutations were made and progeny from each cross were tested for the presence of recombinant phenotypes. The presence of recombinant phenotypes among these progeny (either wild type for both loci or double mutant) is marked as a “+” and indicates lack of linkage between the two mutations being tested. Crosses were the following: RLC4 \times BC72; BC7 \times BC52; RLC4 \times BC81; BC60 \times BC70; BC70 \times S220; and BC52 \times S220.

represented by the mutations in strains MDS250, CY17, CY1228, and S220, the mutants were crossed in all pairwise combinations. This first required crossing each mutant with strain A612 and with strain SWJ298 to obtain a series of strains with complementing genetic markers, the suppressor mutations, and a wild-type *nimX*⁺ allele (Table 1). All possible combinations of crosses of suppressor mutations were carried out, and the progeny were analyzed for the presence of recombinant phenotypes among the suppressor mutations (Table 3). Progeny that were either phenotypically wild type or that possessed both suppressor phenotypes were scored as recombinants. For example, for a cross between BC7 and BC52 (which have the suppressor mutations from MDS250 and CY1228, respectively), both wild-type and DMSO⁻, Cs⁻ progeny were scored as recombinants. In a cross between RLC4 and BC72 (which have mutations from MDS250 and CY17, respectively), both parents were HU-sensitive, so the presence of wild-type progeny alone was used to indicate that the genes are not linked. However, double mutants were identified because they were Cs⁻ and formed extremely small colonies at 32° (not shown). Examination of these strains via fluorescence microscopy confirmed that in addition to being Cs⁻, they have the suppressor phenotype originally identified in CY17 (see Figure 3B). In all crosses, progeny with wild-type and/or double-mutant phenotypes were isolated, indicating that four different genes have been identified.

The four extragenic suppressor mutations identified were designated *snxA1*–*snxD1*, for suppressor of *nimX*. The plate growth phenotypes of strains carrying each of these mutations in the presence and absence of the *nimX2* allele are shown in Figure 1. The cold-sensitive *snxA1* mutation suppresses *nimX2* such that near wild-type growth and normal conidiation are observed in double mutants at 42°, while at 20° colonies do not form. Interestingly, this mutation also confers sensitivity to 15 mM HU. The two mutations originally identified

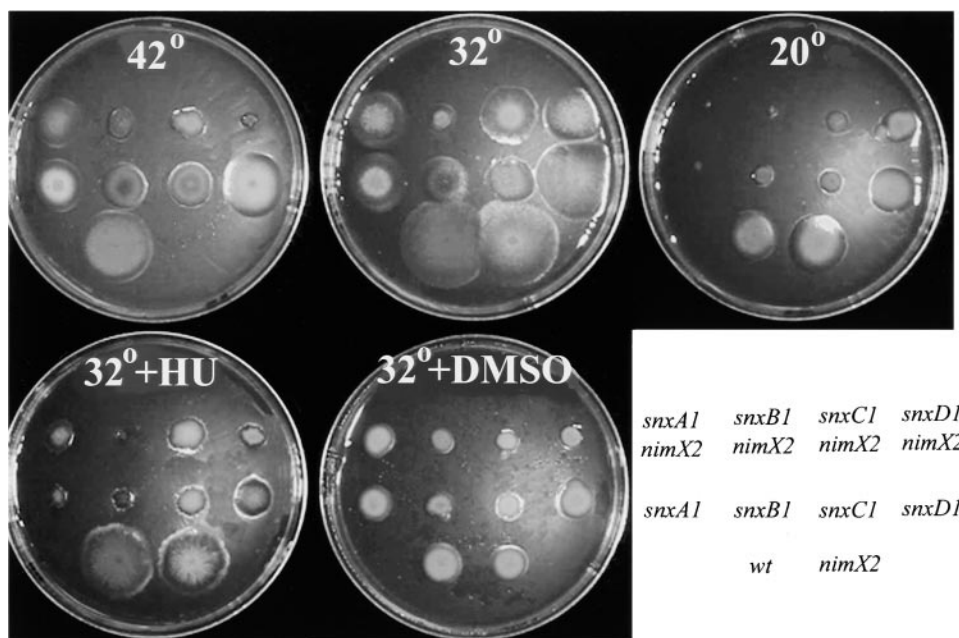


FIGURE 1.—Plate growth phenotypes of suppressor mutations in the presence and absence of the *nimX2* allele. Solid plates MG (top row), MG + 15 mM HU (bottom left), or MG + 4% DMSO (bottom right) plates were point inoculated with spores as follows: top row, double mutants, left to right, MDS250 (*snxA1 nimX2*), CY17 (*snxB1 nimX2*), CY1228 (*snxC1 nimX2*), or S220 (*snxD1 nimX2*); middle row, single mutants, BC7 (*snxA1*), BC70 (*snxB1*), BC52 (*snxC1*), or BC93 (*snxD1*); bottom row, A612 (wild type), SO64 (*nimX2*). Plate incubations were 42°, 3 days (top left); 32°, 3 days (top middle); 20°, 7 days (top right); or 32°, 5 days (bottom row).

as being HU sensitive, *snxB1* and *snxD1*, both partially suppress *nimX2*, allowing double mutants to form small aconidial colonies at 42°. These mutations also lead to small but robustly conidiating colonies at 32° and 20°. Both *snxB1* and *snxD1* strains conidiate normally at 42° and 32° in the absence of the *nimX2* mutation; *snxB1* is unable to form viable colonies in the presence of 15 mM HU, while *snxD1* forms a small colony. The *snxC1* mutation allows partial suppression of heat sensitivity due to the *nimX2* mutation; it produces sparse conidia at 42° and at 32° and is completely aconidial in the presence of 4% DMSO. Colonies of both double (*snxC1 nimX2*) and single (*snxC1*) mutant strains produce long aerial hyphae, which have numerous aberrantly shaped conidiophores extending from them.

Testing for allele specificity of the suppressor mutations: To determine if the *snx* mutations are allele-specific, suppressor strains were crossed to SO69 (*nimX1*) and to SO65 (*nimX3*) and the progeny analyzed for the presence of double-mutant phenotypes (both temperature-sensitive and sensitive to conditions selective for the particular *snx* mutation being analyzed). Cold-sensitive, heat-sensitive progeny were isolated from both SO65 (*nimX3*) × BC16 (*snxA1*) and SO69 (*nimX1*) × BC16 (*snxA1*) crosses, and the resulting double mutants were tested at various temperatures (37°, 41.5°, 43°) to determine if partial suppression occurred. No differences in the heat sensitivity of the progeny were observed compared to the *nimX3* or *nimX1* strains, indicating that *snxA1* is an allele-specific suppressor of *nimX2*. Double mutants were also isolated for SO65 (*nimX3*) × MCG1 (*snxB1*), SO65 (*nimX3*) × BC76 (*snxD1*), and SO69 (*nimX1*) × BC76 (*snxD1*), also with no partial suppression. Double mutants isolated from SO69 (*nimX1*) × MCG1 (*snxB1*) were completely inhibited at 43°, but

exhibited some growth at 42°, indicating that *snxB1* partially suppresses *nimX1*. Despite repeated attempts, crosses between SO65 (*nimX3*) and SO69 (*nimX1*) with *snxC1* strains did not produce viable cleistothecia; thus the allele specificity of *snxC1* could not be determined.

Chromosome mapping and dominance testing: Diploids between mitotic mapping strain A154 and strains containing each of the four suppressor mutations were created to determine the dominant/recessive nature of the mutations and to map each mutation to its specific linkage group. *snxA1*, *snxB1*, and *snxD1* were shown to be recessive, as the diploids exhibited the wild-type phenotype. *snxC1* was classified as partially dominant because the *snxC1/snxC⁺* diploid exhibited the aerial hyphae and sparse conidiation observed in the *snxC1* haploid in the absence of DMSO, but it was able to conidiate in the presence of 4% DMSO, similar to wild type. Parasexual analysis indicated that *snxA* is located on chromosome II, *snxB* is on chromosome VII, *snxC* is on chromosome I, and *snxD* is on chromosome VII.

Testing for allelism of *snxA* and other chromosome II cell cycle genes: Several known cell cycle genes map to chromosome II, as does *nimX^{cdc2}*. These include *nimT^{cdc25}*, *nimE^{cyclinB}*, and *ankA^{wee1}*, which interact with *nimX^{cdc2}*, as well as *nimG* and *nimR*. To determine if *snxA* is allelic with any of these, strains carrying the *snxA1* mutation were crossed to strains with mutations in each of the chromosome II cell cycle genes. In all cases, recombinant progeny with clear double-mutant phenotypes were obtained (Table 4), indicating that *snxA* is a novel cell cycle regulatory gene and that the *snxA1* mutation does not suppress mutations in other known *G₂*-specific genes that interact with *nimX^{cdc2}*.

Phenotypic characterization of the *snx* mutants: Nuclear and hyphal morphologies of each of the *snx* mu-

TABLE 4

Allelism tests between *snxA* and other chromosome II cell cycle regulatory genes

<i>snxA1</i> ×	No. of progeny with phenotype			
	Wild type	<i>snxA1</i>	<i>nim</i> (*)	<i>snxA1/nim</i> (*)
<i>nimE6</i> (<i>cyclinB</i>)	5	31	56	7
<i>nimT23</i> (<i>cdc25</i>)	22	24	27	5
Δ <i>ankA</i> (<i>wee1</i>)	9	17	4	20
<i>nimG10</i> (<i>G1</i>)	11	40	8	9
<i>nimR21</i> (<i>S</i>)	19	42	25	14

Crosses between strains carrying *snxA1* (Cs^-) and mutations in the indicated genes were made and the progeny analyzed for mutant phenotypes. Numbers indicate the number of progeny identified with the phenotype corresponding to the genotype listed at the top of the column. Each of the *nim* mutants tested was temperature-sensitive and progeny were tested at 44° (for the *nim* mutation) and 20° (for *snxA1*). The Δ *ankA* strain is HU-sensitive and progeny were thus tested at 20° and in the presence of 15 mM HU. The existence of both wild-type and double-mutant progeny indicates lack of allelism. *nim** refers to the specific *nim* mutation with which the *snxA1* strains were crossed. Crosses were the following: SWJ198 × BC7; SWJ108 × BC7; SWJ013 × BC7; SWJ313 × BC7; and Δ *ankA* × BC26.

tants were examined by DAPI/calcofluor double staining of hyphae. The *nimX2* mutation alone leads to arrest of the nuclear division cycle in G_1 or G_2 at 42° (OSMANI

et al. 1994). The cells arrest with a single interphase nucleus but exhibit some germ tube extension (Figure 2B). Both single mutants (*snxA1*) and double mutants (*snxA1 nimX2*) have similar phenotypes at all temperatures tested (42°, 32°, 20°). *snxA1 nimX2* double mutants are able to undergo nuclear division and germ tube extension at 42°; however, the majority of the nuclei are smaller than those of wild-type cells (Figure 2C) and the cell wall is swollen in ~25% of both single- and double-mutant cells at 42° ($n = 100$; Figure 2D). The swollen areas may be confined to the conidial head (the part of the germling that corresponds to the original spore) or they may be found as part of the hyphae; in all cases, swollen areas appear to be packed with small interphase nuclei. These nuclei are often obscured in micrographs due to intense DAPI staining. At 32°, both *snxA1 nimX2* and *snxA1* cells (Figure 2F) appear wild type, with only a small percentage (10%) of cells containing swollen areas. Both *snxA1* (Figure 2G) and *snxA1 nimX2* cells arrest in interphase of the cell cycle at 20° with a single nucleus and ungerminated conidia. Although an occasional cell (3%) will undergo a single nuclear division and slight germ tube extension, if allowed to incubate for 2–3 days at 20° these arrest with large, aberrantly shaped, nuclei and swollen hyphae (Figure 2H).

snxB1 nimX2 double mutants exhibit nuclear division and germ tube extension at 42° (not shown). Interest-

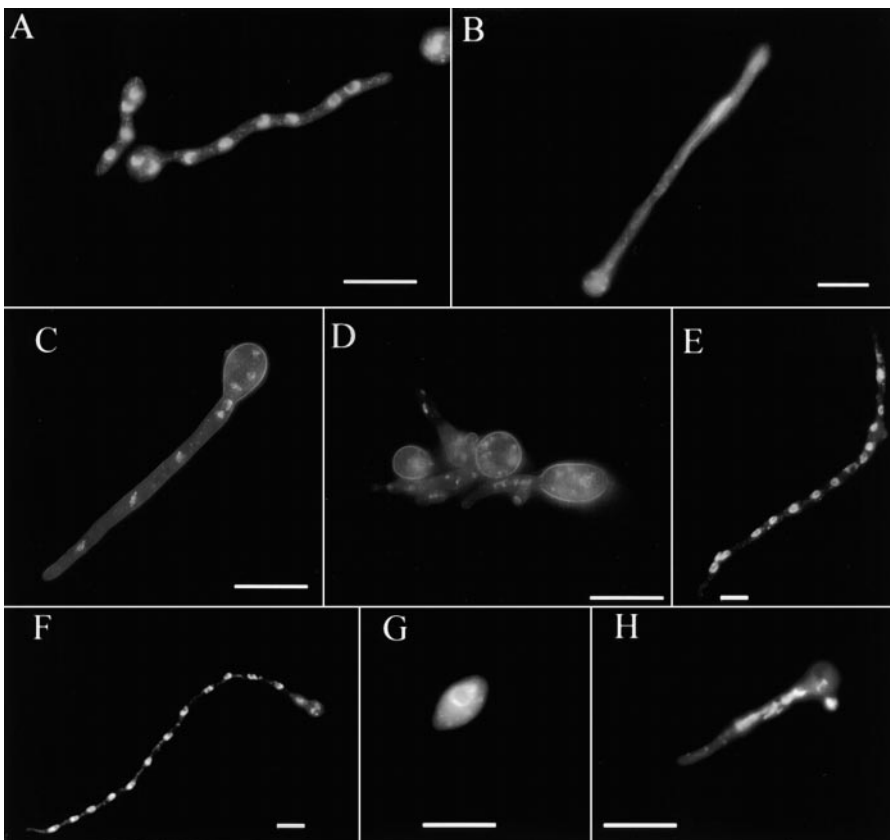


FIGURE 2.—Cellular morphologies of *snxA*⁺, *nimX2*, *snxA1*, and *snxA1 nimX2* germlings. Conidia from strains A612 (*snxA*⁺ *nimX*⁺), SO64 (*nimX2*), RLC1 (*snxA1*), and MDS250 (*snxA1 nimX2*) were inoculated onto coverslips in YG. Coverslips were incubated as indicated below, fixed, and stained with DAPI. Interphase nuclei are identified by diffuse DAPI staining and the presence of prominent nucleoli. (A) A612 incubated at 42° for 8 hr; (B) SO64 incubated at 42° for 16 hr; (C and D) MDS250 incubated at 42° for 16 hr; (E) RLC1 incubated at 42° for 16 hr; (F) RLC1 incubated at 32° for 16 hr; (G) RLC1 incubated at 20° for 25 hr; and (H) RLC1 incubated at 20° for 72 hr. Bars, 5 μm.

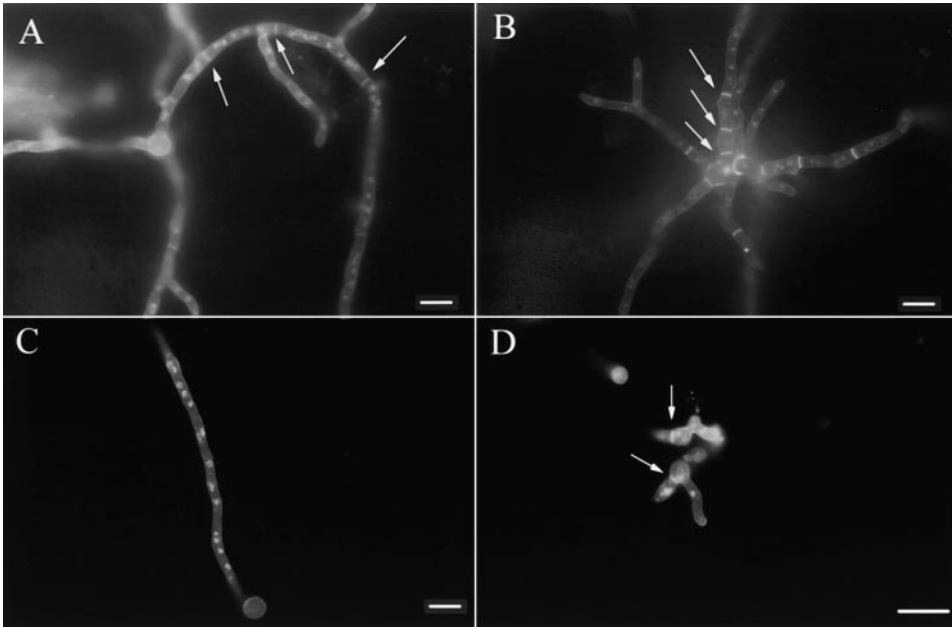


FIGURE 3.—*snxB1* causes increased branching and septation and sensitivity to HU. Conidia from strain A612 (*snxB⁺*; A and C) or strain BC70 (*snxB1*; B and D) were inoculated onto coverslips in YG (A and B) or YG + 15 mM HU (C and D), incubated at 32° for 16 hr, fixed, and stained with DAPI and calcofluor. Arrows indicate septa. Bars, 5 μ m.

ingly, at 32° both *snxB1 nimX2* and *snxB1* cells (Figure 3B) exhibit increased septation compared to wild-type cells (Figure 3A). This same septation pattern is observed in *snxB1* cells at 42° (not shown). The average subapical cell (septum to septum) length in wild-type cells was $21.5 \pm 8.8 \mu\text{m}$, and the average subapical cell length in *snxB1* cells was $7.4 \pm 2.6 \mu\text{m}$, which was determined to be highly statistically significant ($P < 0.01$).

Both *snxB1* and *nimX^{delc2AF}* mutants form hyperseptate hyphae. The *nimX^{delc2AF}* mutation causes cells to form septa earlier than wild-type cells—where wild-type cells do not form septa until eight nuclei are present, *nimX^{delc2AF}* leads to septum formation earlier. To determine if *snxB1* causes early septation, BC72 (*snxB1*), R153 (wild type), and Fry-20-1 (*nimX^{delc2AF}*) conidia were germinated at 32° until the average cell contained four nuclei, and the number of septated cells containing four nuclei was determined. Where 51% of *nimX^{delc2AF}* cells at this stage contained septa, only 4% of *snxB1* cells and 0% of wild-type cells contained septa. This indicates that *snxB1* does not lead to hyperseptation by allowing septa to form earlier than wild-type cells.

In the presence of 15 mM HU, both *snxB1 nimX2* and *snxB1* cells germinate, but the nuclei are small and punctate, and very little germ tube extension occurs (Figure 3D). Septation does not normally occur in wild-type cells until after eight nuclei are present and is inhibited in the presence of 15 mM HU (Figure 3C), but septation and the beginnings of branching are observed in *snxB1* cells in the presence of 15 mM HU.

The *snxC1* mutation suppresses the *nimX2* mutation nearly completely at 42°. In both single and double mutants (Figure 4A), hyphae exhibit normal nuclear division and germ tube extension compared to wild

type (Figure 3A). Formation of the first septum is often displaced such that rather than occurring at the base of the conidial head, it occurs further into the germ tube, but hyphal septa have spacing and morphology similar to wild type. In both *snxC1 nimX2* and *snxC1* strains, conidiation is significantly decreased at all temperatures and long aerial hyphae with aberrantly shaped conidiophores are produced (Figure 4, C–E). Conidiation is completely inhibited in the presence of 4% DMSO. Wild-type conidiophores are radially symmetrical and consist of a stalk with a single vesicle from which multiple primary sterigmata (metulae) bud. From each metula two secondary sterigmata (phialides) usually bud, and these bud multiple times to give rise to long chains of conidia. Conidiophores of *snxC1* strains exhibit a variety of aberrant morphologies. Some *snxC1* conidiophores are normal in appearance, while others have development arrested at various stages or have multiple conidiophore structures extending from the stalk or vesicle (Figure 4E). One frequently observed abnormality is the presence of asymmetric metulae (Figure 4D) that are often unable to form phialides or that begin to form structures resembling hyphae rather than phialides. All aberrantly shaped conidiophores observed contain septa in the conidiophore stalk, and some have septa in the conidiophore head. Wild-type conidiophores do not have septa in the conidiophore stalk and normally stain very calcofluor bright (Figure 4B).

snxD1 only marginally suppresses the *nimX2* mutation, as 36% of *snxD1 nimX2* cells undergo mitosis after 20 hr of incubation at 42° (Figure 5A), whereas 100% of wild-type cells undergo division under these conditions ($n = 100$). *snxD1* strains grow well at 32°, with normal nuclear division and germ tube extension, but with

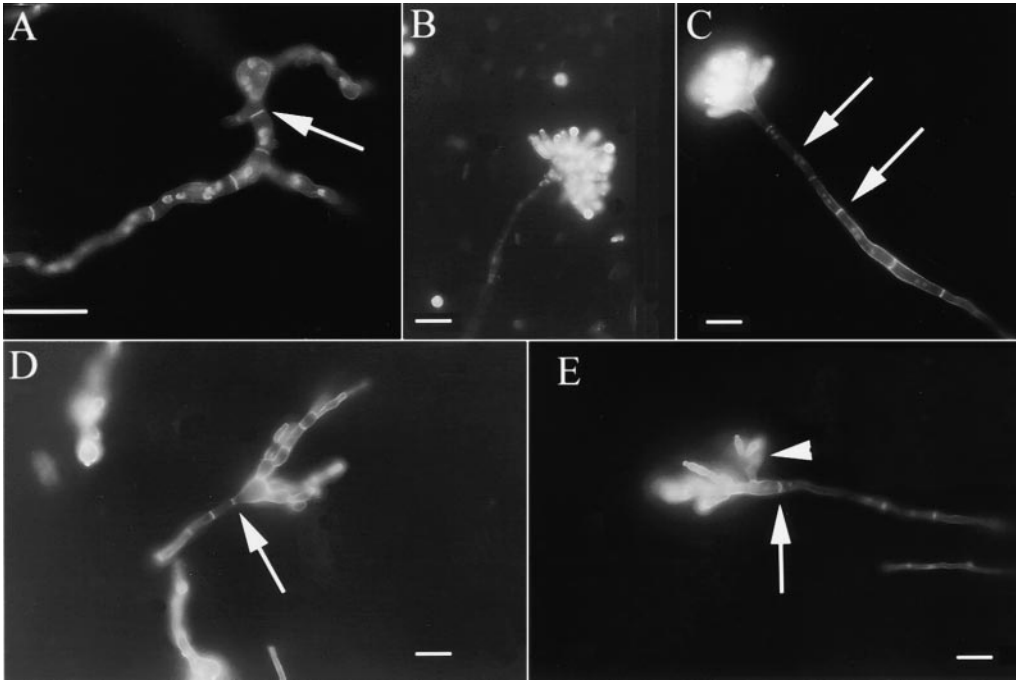


FIGURE 4.—*snxC1* causes septation in the conidiophore stalk. (A) CY1228 conidia (*snxC1 nimX2*) were inoculated onto coverslips in YG and incubated at 42°, 16 hr, fixed, and stained with DAPI and calcofluor. (B–E) A612 (B) or BC64 (*snxC1*; C–E) conidia were inoculated onto MG plates and incubated at 32° for 2 days. To visualize conidiophore structure, conidiophores were harvested into fix and stained with DAPI and calcofluor. Arrows indicate septa. Arrowhead indicates a second conidiophore-like structure. Bars, 5 μ m.

slightly increased septation (Figure 5B) as well as an occasional short, anuclear compartment or double septum (Figure 5C). At 32°, subapical cell length is $12.1 \pm 3.6 \mu\text{m}$ compared to $21.5 \pm 8.8 \mu\text{m}$ for wild type, and this difference was determined to be highly statistically significant ($P < 0.01$). A total of 12% of cells have anuclear compartments or double septa (compared to 1%

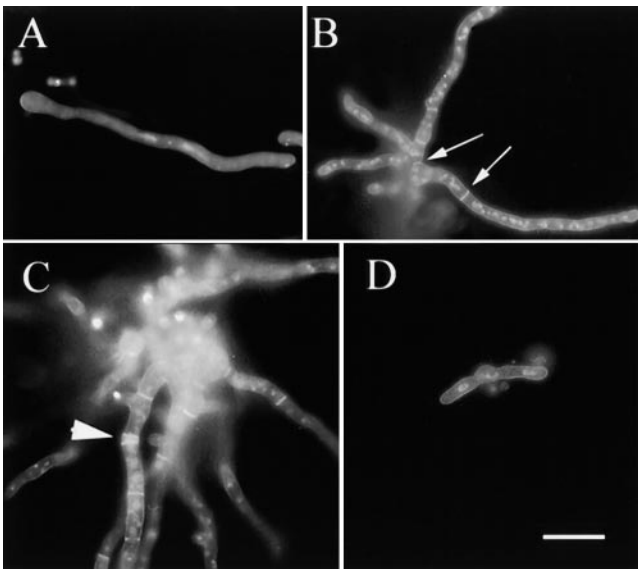


FIGURE 5.—*snxD1* partially suppresses the *nimX2* mutation and causes aberrant septation, closely spaced nuclei, and HU sensitivity. Conidia from strains S220 (*snxD1 nimX2*; A) or BC76 (*snxD1*; B–E) were inoculated onto coverslips in YG, incubated as below, fixed, and stained with DAPI and calcofluor. (A) S220, 42°, 16 hr; (B and C) BC76, 32°, 16 hr; (D) BC76, 32°, 16 hr, + 15 mM HU. Arrows indicate septa; arrowhead indicates a double septum. Bar, 5 μ m.

for wild-type cells; $n = 100$). Both double and single mutants are also sensitive to 15 mM HU. In the presence of HU, cells undergo nuclear division and germ tube extension much more slowly than wild type, but the nuclei appear normal (Figure 5D).

Testing for genetic interactions of *snxB* and *snxC* with *nimT^{cdc25}* and *ankA^{wee1}*: The increased septation and HU sensitivity due to the *snxB* mutation are similar to the effects of deletion of *ankA^{wee1}*, and *snxC1* causes aberrant conidiophores similar to those caused by the *nimX^{cdc2AF}* mutation. This suggests that *snxB* and *snxC* may be involved in the Tyr-15 phosphorylation of NIMX^{CD²}. We therefore wished to determine if either the *snxB1* or *snxC1* mutations interact with genes known to regulate the tyrosine phosphorylation of *nimX^{cdc2}*. Strains carrying the *snxB1* or *snxC1* mutations were crossed to strains carrying mutations in *nimT^{cdc25}* and *ankA^{wee1}*. *snxB1 nimT23^{cdc25}* double mutants grow significantly better than *nimT23^{cdc25}* single mutants under restrictive conditions (42°), indicating that *snxB1* suppresses the *nimT23^{cdc25}* mutation (Figure 6). In contrast to the suppression of *nimT23^{cdc25}* by *snxB1*, *snxB1 Δ ankA^{wee1}* double mutants have a synthetic lethal phenotype. While *Δ ankA^{wee1}* strains are sensitive to 5 mM HU, single mutants can form a colony in the presence of 1 mM HU. The *snxB1 Δ ankA^{wee1}* double mutants are unable to form a colony in the presence of 1 mM HU, similar to *nimX^{cdc2AF}* mutants (data not shown).

Similar analyses indicated that *snxC1* does not suppress *nimT23^{cdc25}* but can partially suppress *Δ ankA^{wee1}*. The *snxC1 nimT23^{cdc25}* double mutants were more heat sensitive than *nimT23^{cdc25}* alone, as *nimT23^{cdc25}* allows some growth at 42° but the *snxC1 nimT23^{cdc2}* double mutants do not (Figure 6). *snxC1 Δ ankA^{wee1}* double mu-

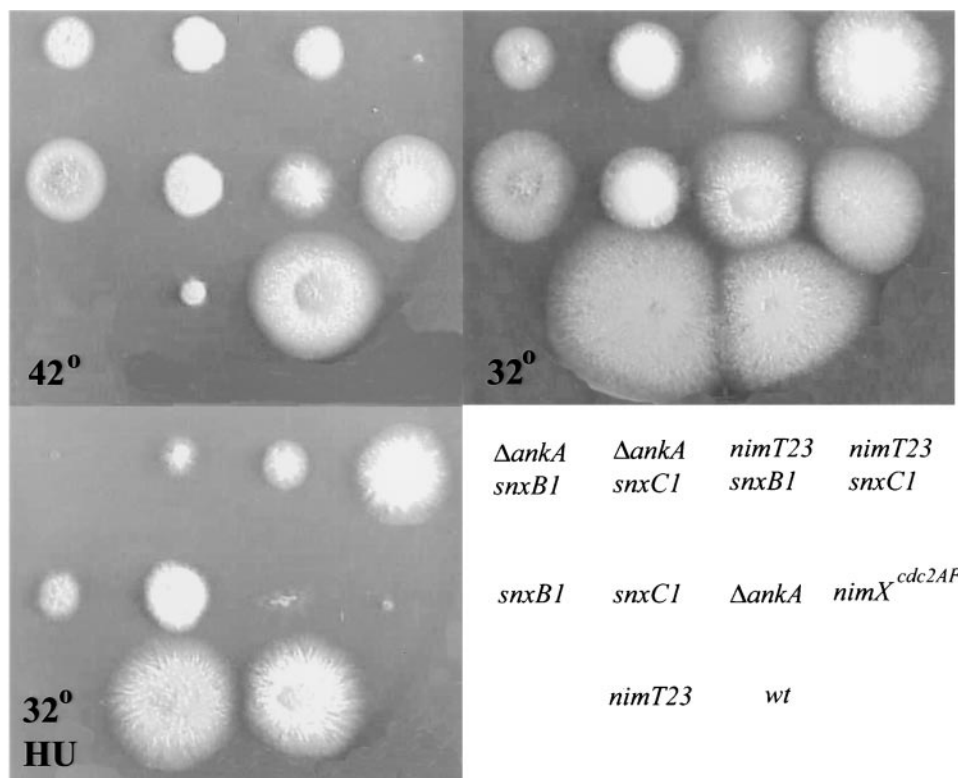


FIGURE 6.—Plate growth phenotypes of *snxB1* and *snxC1* mutations in the presence and absence of $\Delta ankA^{wee1}$ or *nimT23^{cdc25}*. Solid plates MG incubated at 42° (top left) or 32° (top right) or MG + 7 mM HU incubated at 32° (bottom left) were point inoculated with spores as follows: top row, double mutants, left to right, MCG3 ($\Delta ankA$ *snxB1*), MCG4 ($\Delta ankA$ *snxC1*), MCG5 (*nimT23* *snxB1*), MCG6 (*nimT23* *snxC1*); middle row, BC72 (*snxB1*), BC52 (*snxC1*), $\Delta ANKA$, Fry-20-1 (*nimX^{cdc2AF}*); bottom row, SWJ108 (*nimT23*), R153 (wild type). Plate incubations were for 3 days.

tants are able to form a small colony in the presence of 5 mM HU and 7 mM HU, concentrations at which $\Delta ankA^{wee1}$ single mutants were unable to grow. Thus, *snxC1* produces a synthetic lethal phenotype in combination with *nimT23^{cdc25}* but partially suppresses $\Delta ankA^{wee1}$.

***snxA1* causes a nuclear division cycle block in G₁ or early S:** Germination of *snxA1* strains at 20° for 25 hr followed by DAPI staining (Figure 2G) indicated that *snxA1* causes nuclei to arrest in interphase at the restrictive temperature, where wild-type cells normally undergo one to two nuclear divisions under these conditions. That the nuclei were in interphase under these conditions was confirmed by indirect immunofluorescence of microtubules, which exhibited a typical interphase array (data not shown) rather than mitotic spindles. The *snxA1* block is reversible until ~40 hr of incubation at 20°. If incubation is allowed to proceed for 48 hr at 20°, the block becomes irreversible, as abnormal nuclei begin to accumulate (Figure 2H). To determine at which stage of interphase this nuclear division arrest occurs, reciprocal shift assays were performed on strains BC7 (*snxA1*; Table 5) and MDS250 (*snxA1 nimX2*; not shown). Conidia were inoculated into rich media + 25 mM HU and incubated 6.5 hr at 32°, and then shifted to 20° in the absence of HU for 25 hr or shifted to 32° in the absence of HU. After downshift to 20°, 100% of the nuclei underwent mitotic division and then arrested with aberrantly shaped nuclei. This indicates that the cells exit from the S-phase arrest induced by the HU, traverse through G₂ and mitosis, and arrest in G₁ or

early S (at a point before the HU arrest) at the restrictive temperature of 20° (see BERGEN *et al.* 1984). Under these same conditions, either a late S-phase arrest (after the HU arrest point) or a G₂ arrest would lead to undivided nuclei. As a control (not shown) the reciprocal experiment was performed, in which conidia were inoculated onto coverslips in rich media and incubated at 20° for 25 hr, and then shifted to 32° in the presence of 25 mM HU. For this experiment, a block in either G₁ or early S would prevent nuclear division. A total of 85% of the cells contained undivided nuclei following the shift from 20° to 32° + 25 mM HU, suggesting a G₁ or early S block. These experiments were repeated four times, either with strain BC7 or strain MDS250, with similar results. As the first experiment rules out G₂ arrest

TABLE 5

Hydroxyurea shifts of *snxA1* mutants

Shift	% divided	Cells arrest in
32° + HU, 6.5 hr	0	S
32° + HU, 6.5 hr, then 20°, 25 hr, -HU	100	G ₁ or early S
32° + HU, 6.5 hr, then 32°, 16 hr, -HU	100	None

BC7 (*snxA1*) conidia were inoculated onto coverslips in YG and incubated as indicated, fixed, and stained with DAPI. HU concentration was 25 mM. One hundred cells were counted for each experiment and the percentage with one nuclear division was calculated.

or S arrest after the HU arrest point, and the second supports either early S (before the HU arrest point) or G₁ arrest, these data indicate that the *snxAI* nuclear division arrest at 20° occurs either during G₁ or during early S.

DISCUSSION

In an effort to further understand how the NIMX^{CDC2} protein kinase affects nuclear division, septation, and development in *A. nidulans*, we have generated a set of strains containing extragenic suppressors of the temperature-sensitive *nimX2^{cdc2}* mutation. Extragenic suppressor analysis is designed to allow interacting proteins to be identified; thus the suppressors described here represent genes that interact with NIMX^{CDC2}. In addition to suppression of the *nimX2* mutation, mutations in the four suppressor genes, *snxA*, *snxB*, *snxC*, and *snxD*, independently affect nuclear division, septation, and conidiation.

***snxA* is required for progression through G₁ or early S:** Dormant conidia of *A. nidulans* have a single condensed nucleus that enters the cell cycle at G₁ when dormancy is broken. The spores grow isotropically until a critical cell size is reached and then switch to polar growth and begin to undergo nuclear division. Following the first nuclear division, a switch to polarized cell growth occurs as a germ tube emerges from the conidial head. The NIMX^{CDC2} protein kinase has been shown to be required for nuclear division both at G₁ and G₂ in *A. nidulans* (OSMANI *et al.* 1994) as well as for progression through S phase (YE *et al.* 1997a). However, no G₁-specific cyclins or other proteins that might interact with NIMX^{CDC2} during G₁ have been identified in this organism. The findings that the cold-sensitive *snxAI* suppressor of *nimX2* leads to a block in G₁ or early S and that it is allele specific suggest that *snxA* represents an important gene that interacts with NIMX^{CDC2} during G₁ or early S. In addition to its cold sensitivity, the *snxAI* mutation also confers slight HU sensitivity at the permissive temperature of 32°. This suggests that *snxA* may also function during the S-phase checkpoint, possibly as part of the APC/C-dependent checkpoint control mechanism (YE *et al.* 1997a). *snxA* is not allelic with any other previously identified nuclear division regulatory genes located on chromosome II in *A. nidulans* and therefore represents a novel nuclear division regulator in this organism.

It is interesting that at the permissive temperature *snxAI* causes problems in the maintenance of cell polarity, leading to locally swollen regions in the hyphae packed with large numbers of nuclei. MOMANY *et al.* (1999) found that the establishment of hyphal polarity and the maintenance of polarity are separate events and identified several mutants (*swob*, *swoe*, *swog*, and *swoh*) defective in polarity maintenance. The *snxAI* mutation often causes regions similar to those found in the *swo*

mutants, where the cells have switched from polarized growth to isotropic growth. Given that *snxAI* mutants are phenotypically similar to *swo* mutants, it would be interesting to determine if any of the *swo* mutations affect NIMX^{CDC2} activity.

***snxB* is required for proper septation:** Septation in *A. nidulans* is the equivalent of cytokinesis and is triggered by mitosis once a critical cell size has been attained (WOLKOW *et al.* 1996). A high level of NIMX^{CDC2} activity has been shown to be required for septation, as the presence of a mutation in *nimT^{cdc25}* or *nimE^{cyclinB}* causes a delay in septum formation (HARRIS and KRAUS 1998). Additionally, the *nimX^{cdc2AF}* allele, which causes an increase in NIMX^{CDC2} activity due to loss of Tyr-15 regulation, leads to increased septation in both hyphae (HARRIS and KRAUS 1998) and conidiophores (YE *et al.* 1999) and to severe HU sensitivity.

snxB1 leads to increased hyphal septation, in addition to its sensitivity to HU, and appears to lower the threshold cell size required to activate septation. A similar phenotype is observed in strains carrying a deletion in *ankA^{wee1}* (data not shown), although the septation defect is more pronounced in *snxB1* mutants. It is possible that cytokinesis in *snxB1* strains is advanced due to a loss of regulation of Tyr-15 phosphorylation of NIMX^{CDC2}. This activity is normally controlled by *ankA^{wee1}* and *nimT^{cdc25}*; however, both of these genes are located on chromosome II and *snxB* is not located on this chromosome. The findings that *snxB1* is HU sensitive, partially suppresses *nimT23*, and is synthetic lethal with Δ *ankA* support the hypothesis that *snxB* affects Tyr-15 phosphorylation of NIMX^{CDC2}. *snxB* could therefore represent a previously uncharacterized gene in the pathway leading to Tyr-15 phosphorylation of NIMX^{CDC2}, possibly functioning as a “backup” WEE1 kinase.

***snxC* is required for proper asexual development:** In *A. nidulans*, asexual development results in the formation of a radially symmetrical conidiophore structure consisting of a stalk, vesicle, metulae, phialides, and conidia. During conidiophore development, changes in septation and nuclear division occur (MIRABITO and OSMANI 1994) such that septation is suppressed in the conidiophore stalk but is tightly coupled with nuclear division in the conidiophore head. This allows one daughter nucleus to enter each metula and phialide, followed immediately in each structure by septum formation. It also allows a change from vegetative growth to budding growth. The switch from hyphal growth to conidiophore development is controlled by the *brlA* transcriptional regulator (ADAMS *et al.* 1998), which has recently been shown to induce the high level of NIMX^{CDC2} kinase activity required for conidiophore development (YE *et al.* 1999). Interestingly, *snxC1* mutants have phenotypes similar to those of *medA* (AGUIRRE 1993) and *brlA42* (MIRABITO *et al.* 1989) developmental mutants in addition to suppressing *nimX2*, suggesting a

role for *snxC* in the developmental regulation of NIMX^{CDC2}.

In wild-type *A. nidulans*, septation and nuclear division are tightly coupled in the hyphae but are uncoupled in the conidiophore stalk, such that multiple nuclei but no septa are present in the stalk. In the *nimX^{cdc2AF}* strain, septation and nuclear division are not uncoupled in the conidiophore stalk, leading to multiple septa in conidiophore stalks and aberrantly shaped conidiophore structures. This suggests that regulation of tyrosine phosphorylation of NIMX^{CDC2} is involved in uncoupling septation from nuclear division in the conidiophore stalk (YE *et al.* 1999). The *snxC1* mutation phenocopies the *nimX^{cdc2AF}* mutation in that it affects septation and cell pattern formation during conidiophore development and in that its effects on conidiation are partially dominant. Because *snxC1* strains do not exhibit abnormal septation in the hyphae, it is possible that *snxC* encodes a development-specific regulator that inhibits the septation promoted by NIMX^{CDC2} activity and that the *snxC1* mutation causes a loss of this regulation, leading to aberrant septation and conidiophore structure. The loss of regulation of Tyr-15 phosphorylation of NIMX^{CDC2} observed in the *nimX^{cdc2AF}* strain is dominant, and any mutation that leads to such a loss of regulation is also likely to be dominant. Because *snxC1* is dominant, phenocopies the conidiophore defects caused by the *nimX^{cdc2AF}* mutation, and partially suppresses $\Delta ankA^{wee1}$, it is likely that it encodes a development-specific protein that regulates Tyr-15 phosphorylation of NIMX^{CDC2}.

***snxD* affects hyphal septation:** The *snxD1* mutation causes HU sensitivity and leads to defects in septation in the absence of HU. The average subapical cell size is 40% shorter than that of wild-type cells, and 12% of the cells have short anuclear compartments or double septa. *snxD1* strains were unable to cross with either *nimT23* or $\Delta ankA$ strains, making an assessment of possible effects on Tyr-15 phosphorylation difficult. The HU sensitivity of the *snxD1* mutation suggests that *snxD* may be involved in or controlled by the S-phase checkpoint function of NIMX^{CDC2}.

This work has identified four genes in *A. nidulans* that interact with the NIMX^{CDC2} cell cycle regulatory protein kinase, each of which has distinct effects on the life cycle of the organism. While much is understood regarding the G₂/M function of NIMX^{CDC2}, little is known about how NIMX^{CDC2} participates in G₁/S, septation, or conidiophore development. The identification of the *snx* genes, which suppress the *nimX2* mutation and also affect these processes, genetically implicates these genes in this participation. Each of these genes is likely to be involved in the upstream regulation of NIMX^{CDC2} activity. Cloning of the genes and biochemical analysis will allow a better understanding of the regulation of nuclear division in *A. nidulans* as well as how the NIMX^{CDC2} master cell cycle regulator affects septation and conidiophore development.

We thank Dr. Stephen A. Osmani for gifts of strains, insightful suggestions, and constructive criticisms, Dr. Peter Mirabito for constructive criticisms of the manuscript, Dr. Steve James for gifts of strains and insightful discussions, and Dr. Greg Leno for use of microscopy facilities. This work was supported by grants from the University of Mississippi Medical Center Chapter of Sigma Xi, the National Beta Beta Beta Foundation, the Millsaps College Faculty Development Fund, the George I. Alden Trust, ChemFirst, and the National Institutes of Health grant R15GM55885 to S.L.M.

LITERATURE CITED

- ADAMS, T. H., J. K. WEISER and J.-H. YU, 1998 Asexual sporulation in *Aspergillus nidulans*. *Microbiol. Mol. Biol. Rev.* **62**: 35–54.
- AGUIRRE, J., 1993 Spatial and temporal controls of the *Aspergillus brlA* developmental regulatory gene. *Mol. Microbiol.* **8**: 211–218.
- BERGEN, L., A. UPSHALL and N. R. MORRIS, 1984 S-phase, G₂, and nuclear division mutants of *Aspergillus nidulans*. *J. Bacteriol.* **159**: 114–119.
- DE SOUZA, C. P. C., X. S. YE and S. A. OSMANI, 1999 Checkpoint defects leading to premature mitosis also cause endoreduplication of DNA in *Aspergillus nidulans*. *Mol. Biol. Cell* **10**: 3661–3674.
- ENGLE, D., 1997 Extragenic suppression: a research method in genetics for undergraduates. *Am. Biol. Teach.* **60**: 297–306.
- FIDDY, C., and A. P. J. TRINCI, 1976 Mitosis, septation, branching and the duplication cycle in *Aspergillus nidulans*. *J. Gen. Microbiol.* **97**: 169–194.
- GLOTZER, M., A. W. MURRAY and M. W. KIRSCHNER, 1991 Cyclin is degraded by the ubiquitin pathway. *Nature* **349**: 132–138.
- HARRIS, S. D., and P. R. KRAUS, 1998 Regulation of septum formation in *Aspergillus nidulans* by a DNA damage checkpoint pathway. *Genetics* **148**: 1055–1067.
- HARRIS, S. D., J. L. MORRELL and J. E. HAMER, 1994 Identification and characterization of *Aspergillus nidulans* mutants defective in cytokinesis. *Genetics* **136**: 517–532.
- HOLT, C. L., and G. S. MAY, 1996 An extragenic suppressor of the mitosis-defective *bimD6* mutation of *Aspergillus nidulans* codes for a chromosome scaffold protein. *Genetics* **142**: 777–787.
- KAFER, E., 1977 Meiotic and mitotic recombination in *Aspergillus* and its chromosomal aberrations. *Adv. Genet.* **19**: 33–131.
- KAMINSKYJ, S. G., and J. E. HAMER, 1998 *hyp* loci control cell pattern formation in the vegetative mycelium of *Aspergillus nidulans*. *Genetics* **148**: 669–680.
- LIES, C. M., J. CHENG, S. W. JAMES, N. R. MORRIS, M. J. O'CONNELL *et al.*, 1998 BIMA^{APC3}, a component of the *Aspergillus* anaphase promoting complex/cyclosome, is required for a G₂ checkpoint blocking entry into mitosis in the absence of NIMA function. *J. Cell Sci.* **111**: 1453–1465.
- MACNEILL, S. A., J. CREANOR and P. NURSE, 1991 Isolation, characterization and molecular cloning of new mutant alleles of the fission yeast p34^{cdc2+} protein kinase gene: identification of temperature-sensitive G₂-arresting alleles. *Mol. Gen. Genet.* **229**: 109–118.
- MIRABITO, P. M., and S. A. OSMANI, 1994 Interactions between the developmental program and cell cycle regulation of *Aspergillus nidulans*. *Dev. Biol.* **5**: 139–145.
- MIRABITO, P. M., T. H. ADAMS and W. E. TIMBERLAKE, 1989 Interactions of three sequentially expressed genes control temporal and spatial specificity in *Aspergillus* development. *Cell* **57**: 859–868.
- MOMANY, M., P. J. WESTFALL and G. ABRAMOWSKY, 1999 *Aspergillus nidulans swo* mutants show defects in polarity establishment, polarity maintenance and hyphal morphogenesis. *Genetics* **151**: 557–567.
- OSMANI, S. A., and X. S. YE, 1996 Cell cycle regulation in *Aspergillus* by two protein kinases. *Biochem. J.* **317**: 633–641.
- OSMANI, A. H., S. A. OSMANI and N. R. MORRIS, 1990 The molecular cloning and identification of a gene product specifically required for nuclear movement in *Aspergillus nidulans*. *J. Cell Biol.* **111**: 543–551.
- OSMANI, A. H., N. VAN PEIJ, M. MISCHKE, M. J. O'CONNELL and S. A. OSMANI, 1994 A single p34^{cdc2} protein kinase (encoded by *nimX^{cdc2}*) is required at G₁ and G₂ in *Aspergillus nidulans*. *J. Cell Sci.* **107**: 1519–1528.

- PONTECORVO, G., J. A. ROPER, C. M. HEMMONS, K. D. MACDONALD and A. W. J. BUFTON, 1953 The genetics of *Aspergillus nidulans*. *Adv. Genet.* **5**: 141–238.
- PU, R. T., and S. A. OSMANI, 1995 Mitotic destruction of the cell cycle regulated NIMA protein kinase of *Aspergillus nidulans* is required for mitotic exit. *EMBO J.* **14**: 995–1003.
- SATTERWHITE, L. L., and T. D. POLLARD, 1992 Cytokinesis. *Curr. Opin. Cell Biol.* **4**: 43–52.
- SATTERWHITE, L. L., M. J. LOHKA, K. L. WILSON, T. Y. SCHERSON, L. J. CISEK *et al.*, 1992 Phosphorylation of myosin-II regulatory light chain by cyclin-p34^{cdc2}: a mechanism for the timing of cytokinesis. *J. Cell Biol.* **118**: 595–605.
- WOLKOW, T. D., S. D. HARRIS and J. E. HAMER, 1996 Cytokinesis in *Aspergillus nidulans* is controlled by cell size, nuclear positioning and mitosis. *J. Cell Sci.* **109**: 2179–2188.
- WOLKOW, T. D., P. M. MIRABITO, S. VENKATRAM and J. E. HAMER, 2000 Hypomorphic *bimA^{APC3}* alleles cause errors in chromosome metabolism that activate the DNA damage checkpoint blocking cytokinesis in *Aspergillus nidulans*. *Genetics* **154**: 167–179.
- WU, L., S. A. OSMANI and P. M. MIRABITO, 1998 A role for NIMA in the nuclear localization of cyclin B in *Aspergillus nidulans*. *J. Cell Biol.* **141**: 1575–1585.
- YE, X., and S. A. OSMANI, 1997 Regulation of p34^{cdc2}/cyclinB H1 and NIMA kinases during the G2/M transition and checkpoint responses in *Aspergillus nidulans*. *Prog. Cell Cycle Res.* **3**: 221–232.
- YE, X., R. R. FINCHER, A. TANG, K. O'DONNELL and S. A. OSMANI, 1996 Two S-phase checkpoint systems, one involving the function of both BIME and Tyr15 phosphorylation of p34^{cdc2}, inhibit NIMA and prevent premature mitosis. *EMBO J.* **15**: 3599–3610.
- YE, X., R. R. FINCHER, A. TANG and S. A. OSMANI, 1997a The G2/M DNA damage checkpoint inhibits mitosis through Tyr15 phosphorylation of p34^{cdc2} in *A. nidulans*. *EMBO J.* **16**: 182–192.
- YE, X., R. R. FINCHER, A. TANG, K. MCNEAL, S. GYGAX *et al.*, 1997b Proteolysis and tyrosine phosphorylation of p34/cyclin B. *J. Biol. Chem.* **272**: 33384–33393.
- YE, X., R. R. FINCHER, A. TANG, A. OSMANI and S. A. OSMANI, 1998 Regulation of the anaphase-promoting complex/cyclosome by *bimA^{APC3}* and proteolysis of NIMA. *Mol. Biol. Cell* **9**: 3019–3030.
- YE, X., S.-L. LEE, S. L. MCGUIRE, J. E. HAMER, G. C. WOOD *et al.*, 1999 Interaction between developmental and cell cycle regulators is required for morphogenesis in *Aspergillus nidulans*. *EMBO J.* **18**: 6994–7001.
- ZACHARIEA, W., and K. NASMYTH, 1999 Whose end is destruction: cell division and the anaphase-promoting complex. *Genes Dev.* **13**: 2039–2058.

Communicating editor: M. D. ROSE